Journal of Ultrafine Grained and Nanostructured Materials
Vol.48, No.2, December 2015, pp.125-132
https://jufgnsm.ut.ac.ir
Print ISSN: 2423-6845 Online ISSN: 2423-6837
DOI: 10.7508/jufgnsm.2015.02.007

The effect of temperature and strain rate on elongation to failure in nanostructured Al-0.2wt% Zr alloy fabricated by ARB process

Hanieh Solouki[1], Ehsan Borhani[1*] and Mohammadreza Toroghi Nezhad[2]

1. Department of Nano Technology, Nano Materials Engineering Group, Semnan University, Semnan, Iran

2. Department of Material Engineering, Isfahan University of Technology, Isfahan, Iran

Recieved 20 December 2015; Accepted 31 January 2016
[*] *Corresponding author Email : e.borhani@semnan.ac.ir*

Abstract
A nano/ultra-fine grain Al-0.2wt% Zr alloy was produced by accumulated roll bonding (ARB) process after 10 cycles. The fraction of high angle grain boundaries increased from 8% to 65.4% during 10 passes during ARB process. This alloy was subjected to tensile test at different temperatures (523,573 and 623 K) and strain rates (0.1 and 0.01 s^{-1}). The optimum condition of temperature and strain rate of 623k and 0.01s^{-1} was achieved for maximum elongation to failure, leading to 100% elongation, although maximum elongation was achieved at higher strain rate and maximum chosen temperature. In fracture surfaces after the test, dimples in higher temperature were deeper, bigger, and longer than low temperature. Because of presenting the superplasticity character at elevated temperature and higher strain rate, there was no evidence of necking after failure.

Keywords: *elongations, strain rates, temperature, tensile test, ultra-fine grain.*

1. Introduction

Polycrystalline materials with grain size less than 1.0μm are defined as ultrafine-grained (UFG) materials. Many researchers showed that UFG materials have capability of exhibiting a range of superior properties, such as improved toughness within high strength and exceptional magnetic properties. The UFG metals are achieved through the use of various techniques which involve application of severe plastic deformation (SPD) [1]. Different kinds of SPD processes, such as equal-channel angular pressing (ECAP), high-pressure torsion (HPT), cyclic extrusion and compression (CEC), and accumulative roll-bonding (ARB) have been developed for realizing bulk nanostructured metals [2, 3].

Those SPD processes that applied to metals led to elongated grain along the principle deformation direction; also with applying SPD processes to metals, elongated grain (along the principle deformation direction) in microstructure achieved [4-6]. The UFG materials obtained by the SPD processes exhibited high strength which is 2-4 times higher than that of the coarse grained materials. High density of grain boundaries in these metals led to thermally instable [1, 5].

Among these techniques, the ARB is the process for continuous production of sheet

materials using rolling deformation in principle. On laboratory scale, the ARB does not have any limitation on applying various kinds of metals and alloys and has succeeded in producing bulky sheets having nanostructures [4].

The tensile test is applied to measurement of elongation to failure of alloys. In this test, working conditions such as kind of SPD process [3], numbers of cycles in this process [7], the temperature and the strain rate in test [8-11], and type and amount of additional different elements to material [6, 10, 11] are important. These factors can change the results of test and there are many articles about these effective factors in elongation [6-11].

Also, it is known that small amount of Zr added to alloys often improves some properties through thermally stabilizing the microstructures in Al alloys. Adding solid solution elements such as scandium (Sc) or zirconium (Zr) to Al alloys could form precipitates within the matrix and inhibited grain boundary mobility and therefore serves to retain the ultrafine grain sizes [5, 6]. This alloys also showed the elongated UFG structure, good thermal instability at elevated temperature and good hardness [6]. The aim of this study is to investigate the effect of strain rate and temperature on tensile testing of an Al-0.2%wt Zr alloy after 10 ARB cycles in order to find optimum strain rate and temperature to achieving maximum elongation.

2. Materials and Methods

An Al-0.2wt%Zr alloy is used as starting materials in this study. The specimens were homogenized and cold-rolled by 90% reduction in thickness and were cut into sheets with thickness of 2 mm, width of 60 mm, and length of 200 mm. The sheets were solution treated (ST) at 913 K for 86.4 ks and immediately water-quenched. The ST sheets were firstly cold-rolled by 50% reduction in thickness. This procedure is considered as the first cycle of ARB process with lubrication condition and ambient temperature. The rolling speed was 2.0 m/min using a two-high mill with 310 mm diameter rolls, and, for preventing the phase transformation at elevated temperature during rolling, the cold-rolled sheet was cooled into water immediately.

The same roll-bonding conditions were used in the subsequent ARB process. Then cold-rolled sheets with 1 mm thickness were cut into half length, and then the contact surfaces of the sheets where degreased by acetone and wire-brushed by a stainless steel wire-brush. Two pieces of the sheets were stacked to be 2 mm thick and roll bonded by 50% reduction under the same conditions described above. The roll-bonded sheet was immediately cooled into water. This procedure is considered as the second ARB cycle. The ARB procedures were repeated up to 10 cycles (total equivalent strain of 8.0) [4, 5]. The principle of the ARB process is schematically illustrated in Figure 1.

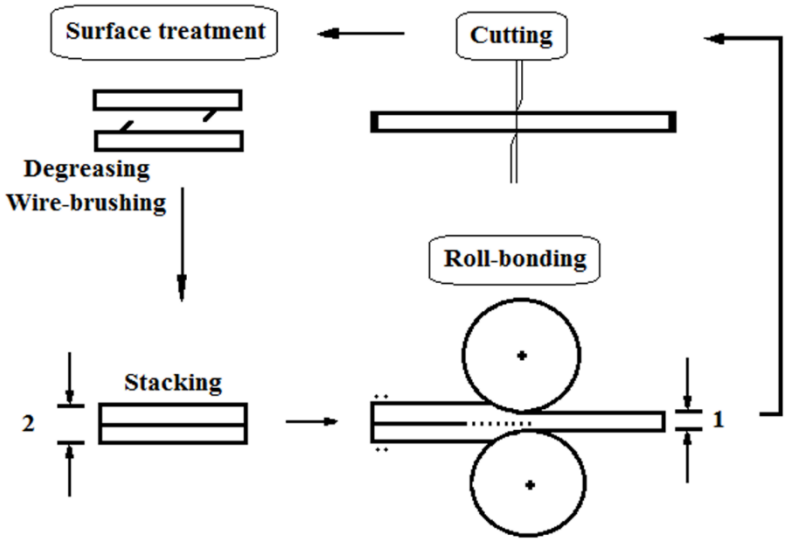

Fig. 1. Schematic illustration showing the principle of the accumulative roll-bonding (ARB) process

The tensile test of the ARB processed specimens was prepared according to ASTM E8 standard and then a hole was created on two ends of samples to fix them to the fixture. Samples were subjected to tensile test at three different temperatures (523, 573 and 623 K) that are below half of melting temperature of the alloy and two common strain rates (0.1 s^{-1} and 0.01 s^{-1}) in order to measure the elongation and find optimum condition. These strain rates are chosen according to the papers that reported about the effective factors on elongation [6-11].

Sections normal to the transverse direction (TD) of the ARB processed specimens were used for the microstructural observations. Electron backscattering diffraction (EBSD) analysis was carried out in a scanning electron microscope (SEM) with a field emission type gun (FE-SEM; Philips XL30) operated at 15 kV using a step size of 0.05 μm. The specimens were mechanically polished and then electro-polished in a solution of 30% HNO_3 and 70% CH_3OH before the measurements. The fracture behavior of the specimens was also studied using SEM technique.

3. Results and Discussion

Electron backscatter diffraction micrograph of the Al-0.2%wt Zr alloy after 10 cycles of ARB process is shown in Figure 2. Nanostructure/ultrafine grains elongated (longitudinal) along rolling direction (RD) are observed in Figure 2(a). The mean grain size of 400 nm is achieved. It can be said that, during ARB process, at low strain, dislocations form banded sub grain structure and finally UFG structure is developed with array of elongated grains that are separated by HAGBs and LAGBs which are indicated with red and green lines in Figure 2(a), respectively [8, 12-13]. The volume fraction of LAGBs and HAGBs are shown in Figure 2(b). In fact, while the strain increases during ARB process, accumulation of dislocation is caused due to increasing the energy in LAGBs, leading to creation of more stabilized HAGBs. As shown in Figure 2(b) and (c), in 10 cycles ARB processed specimen almost 70 % of microstructure is consisted of HAGBs.

The ARB processed specimens after tensile test, conducted at three different temperatures (523, 573, and 623 K) with two strain rates of (a) 0.1 s^{-1} and (b) 0.01 s^{-1}, is shown in Figure 3. This figure indicates the effect of temperature and strain rate on elongation to failure of the specimens. Localization of plastic deformation resulting in the fracture is observed in these specimens. No evidence of necking in samples is observed during the test.

The elongation value for the tensile tested specimens at three different temperatures (523, 573, and 623 K) and initial strain rate of 0.1 s^{-1} and 0.01 s^{-1}, are shown in Figure 4. As can be seen, the total elongation increased as temperature increased and the maximum elongation in each strain rate is happened at 623 K temperature. It is in accordance with literature that the maximum elongation should probably be achieved at highest temperature and maximum strain rate [7, 14-16]. As shown in this figure, not so much difference is observed for temperatures of 573 K and 623 K, although there is the obvious difference in elongation at these temperatures in slower strain rate (0.01 s^{-1}). Almost the same value of elongation was observed for 523 K and 573 K in higher strain rate (0.1 s^{-1}). As a result, temperature and strain rate were effective on elongation to failure in tensile test.

At low temperature, specimens have higher strength and need more force to break because flow in material is difficult at this temperature. As temperature increased, mobility of boundaries was easier and strength decreased [10, 13-14, 17- 23] and elongation increased. Therefore, failure occurred at higher extension.

The stress vs. strain for tensile test specimens at strain rate of 0.1 s^{-1} and 0.01 s^{-1} and different temperatures is shown in Figure 5. According to the results, at higher strain rate (0.1 s^{-1}), strength is higher than that in low strain rate in all temperatures. It can be said that at higher strain rates the material does not have enough time to flow and slide grain boundaries, therefore, lower elongations occur [7, 16]. It is clear that at elevated temperatures the grains in polycrystalline metals are able to move relative to each other and grain boundary sliding occurs in the direction of the grain boundary. It is promoted by increasing the temperature and/ or decreasing the strain rate [24].

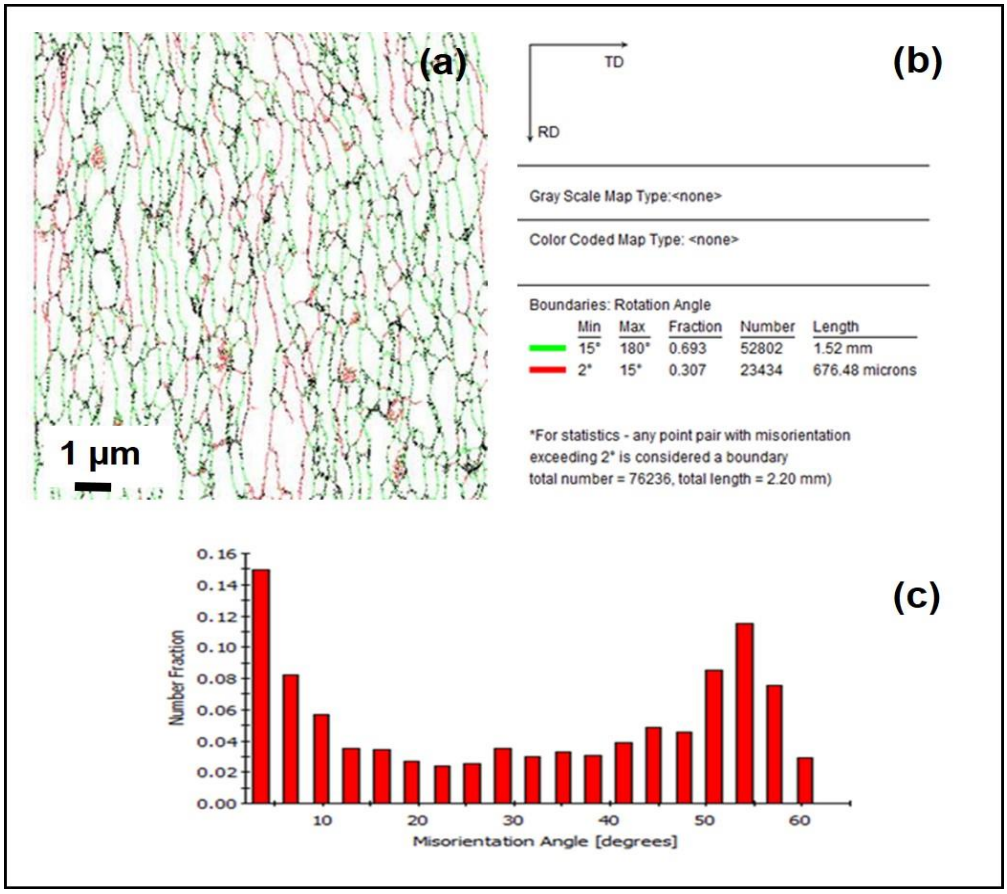

Fig. 2. EBSD image of Al-0.2%wt Zr alloy after 10 ARB cycles. a) The EBSD micrograph, b) rolling direction and volume fraction of LAGBs and HAGBs, c) The misorientation angle distribution

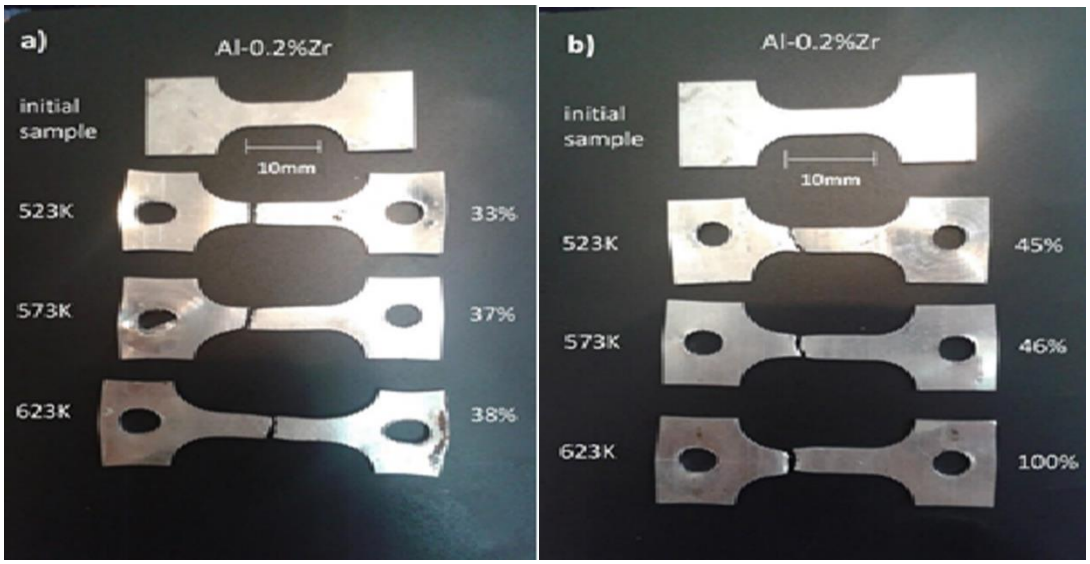

Fig. 3. The 10 cycles ARB processed specimens after tensile test at different temperatures and two strain rates of a) 0.1 s^{-1} and b) 0.01 s^{-1}

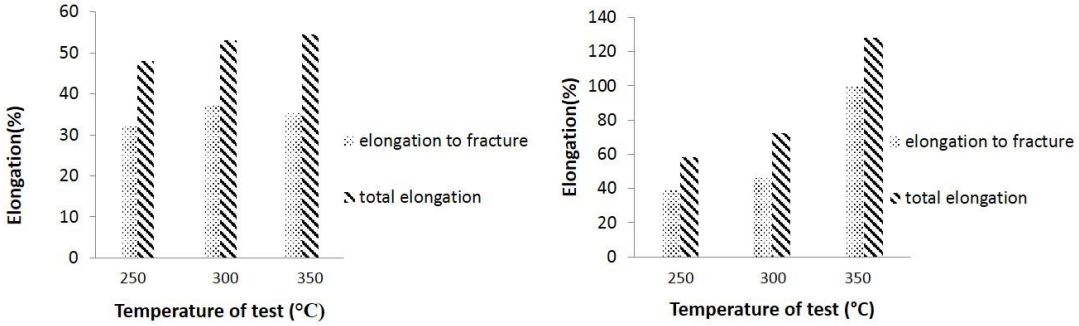

Fig. 4. Results of tensile test at three temperatures (523.573 and 623 K) and a constant strain rate of (a) 0.1 S^{-1} (up) and (b) 0.01 S^{-1} (down) of Al-0.2%wt Zr alloy after 10 cycles ARB

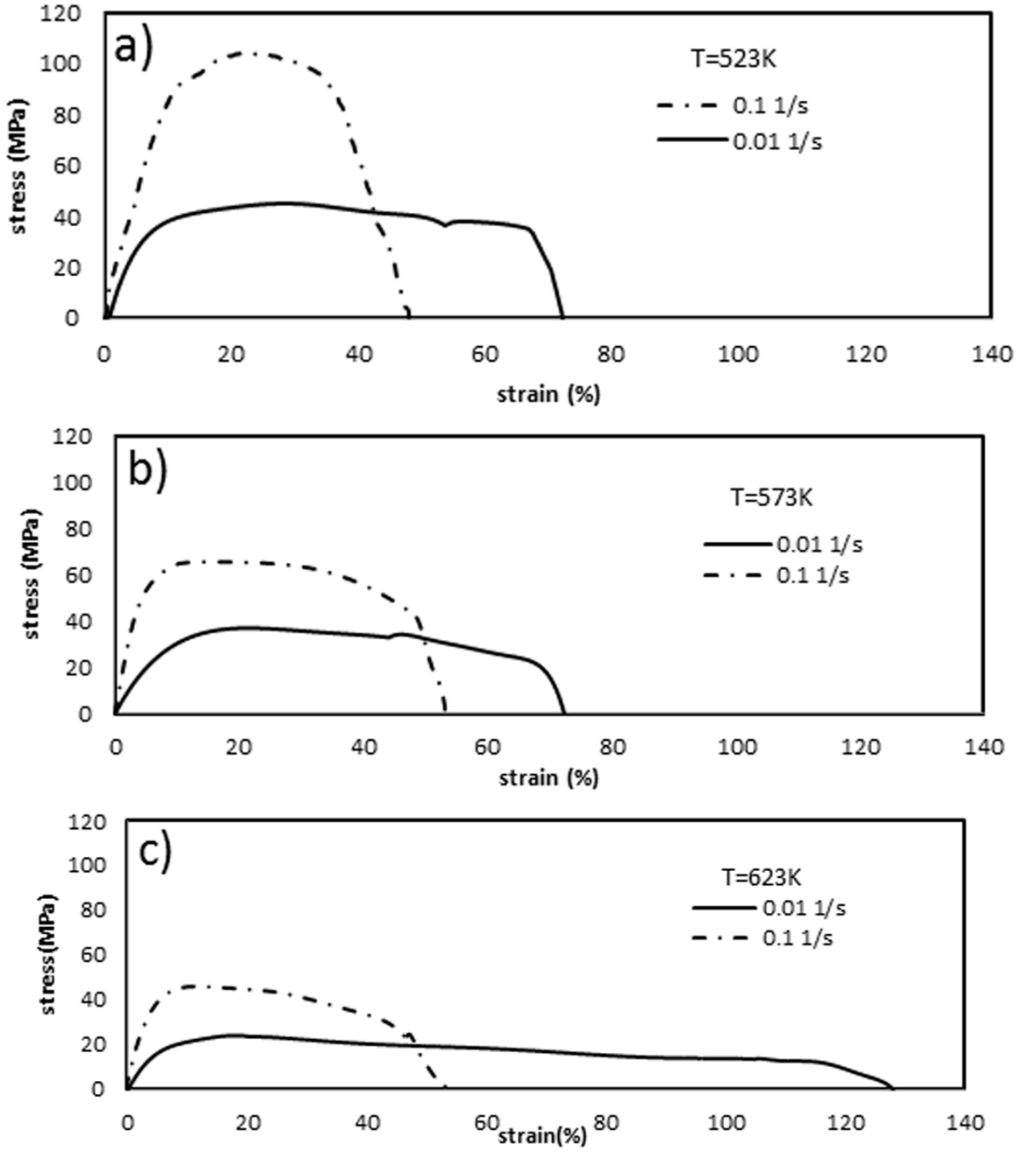

Fig. 5. Results of tensile test at two different strain rate of 0.1 S^{-1} and 0.01 S^{-1} at same temperature a) 523K, b) 573K and c) 623K of Al-0.2%wt Zr alloy after 10 cycles ARB

It has also been concluded that the strain rate is more effective than temperature on elongation. Also, it is clear that more elongation is observed in lower strain rate. The same tendency has been reported in previous studies [1, 6, 7, 10].

The plastic instability condition, i.e. necking criteria, is expressed as following equation [4]:

$$\sigma \geq \frac{\partial \sigma}{\partial \varepsilon} \quad (1)$$

Here, σ and ε are true stress and true strain. The grain refinement increased the flow stress, especially the yield strength of the material [2, 4, 12-13]. However, strain hardening is not enhanced by grain refinement. As a result, plastic instability expressed in equation 1 is easily achieved in UFG materials. Also, in order to manage both high strength and ductility in nanostructured metals, a good balance between strength and ductility is needed which it has been reported in multiphase nanostructure metals and alloys [1, 3-5].

During tensile test, the high density of dislocations induced dynamic recovery and UFG materials exhibited work softening immediately after yielding, leading to plastic instability and the onset of necking [14]. On the other hand, grain refining led to increase in strain rate and decrease in the temperature which super plasticity appeared [25, 26]. The SPD process originally developed by Segal et al. [27, 28] is an effective process to achieve superplastic conditions [29-31]. Typically, grain refinement produces materials that are capable of exhibiting unusual physical and mechanical properties [32-36].

In all graphs of tensile test, a short region of strain hardening is followed by a long region of strain hardening. The same type diagrams can be observed in previous studies [3-4, 16-17, 18-23].

In high temperature, grain growth in nanostructured metals led to premature fracture in tensile test. It has been reported previously that coherent, metastable, and cubic Al_3Zr precipitates form at the mentioned temperatures [5, 15]. Those precipitates prevent grain growth, therefore elongation to failure increases [10, 16-20, 37-38].

The SEM micrographs of the fracture surface of the specimens are shown in Figure 6 and Figure 7. The SEM micrograph of the fracture surface after tensile test at strain rate of 0.1 s^{-1} at different temperatures of 523 K, 573 K, and 623 K is shown in Figure 6. As shown in this figure, observed dimples, created by grain boundary sliding, in structure have different depth and size at different temperatures. There was no evidence of necking in specimens after test. Also, in high temperature, dimples were deeper, bigger, and longer than low temperature which may be attributed to presence of precipitates at those temperatures [5, 15]. Also, these dimples were bigger than the same ones in higher strain rate.

On the other hands, the main import of grain boundary sliding is on the initiation of grain boundary fracture. It should be noted that since the grain boundary sliding is the chief deformation mode, those grain boundaries should be mobile HAGBs to promote sliding [24].

Normally, there are nucleation and growth of some cavities in condition of superplasticity (high temperature and high strain rate), but this growth and void coalescence depends on the size of the cavities [24]. Cavitation is also an important mechanism in tensile process. Cavity nucleation and, after that, micro cavities are deformed at optimum testing condition. During pulling the material, micro cavities developed, initiated by grain boundary sliding [24]. Interlinkage of cavities in the direction of transverse to the tensile axis gives rise to fracture in small elongation [14].

In fast strain rate (0.1 s^{-1}), cavity growth can be prevented to restrict fracture at high temperatures, leading to higher elongation value than lower strain rate (0.01 s^{-1}). Finally, it can be said that, the grain boundary sliding led to fracture by creating or helping to create cavities and dimples. However, condition of test (temperature or strain rate) or chemical composition of material (second phase particle/precipitation) can affect the mechanism of coalescence of cavity and fracture [24, 39, 40].

At last, as shown in Figure 7, maximum elongation observed at 0.01 s^{-1} strain rate and 623 K temperature (100%), showing failure with more and longer dimples.

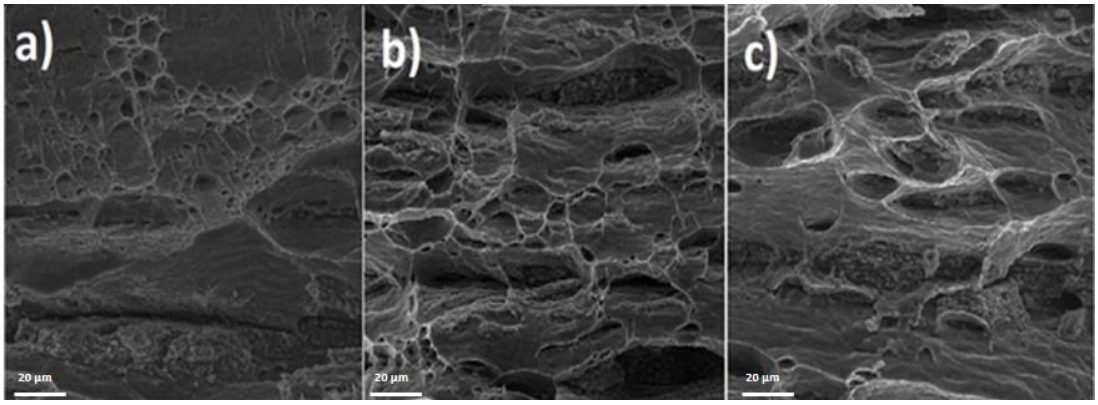

Fig. 6. SEM micrograph of the fracture surface after tensile test at strain rate of 0.1 S^{-1} at different temperatures a) 523K, b) 573K, and c) 623K

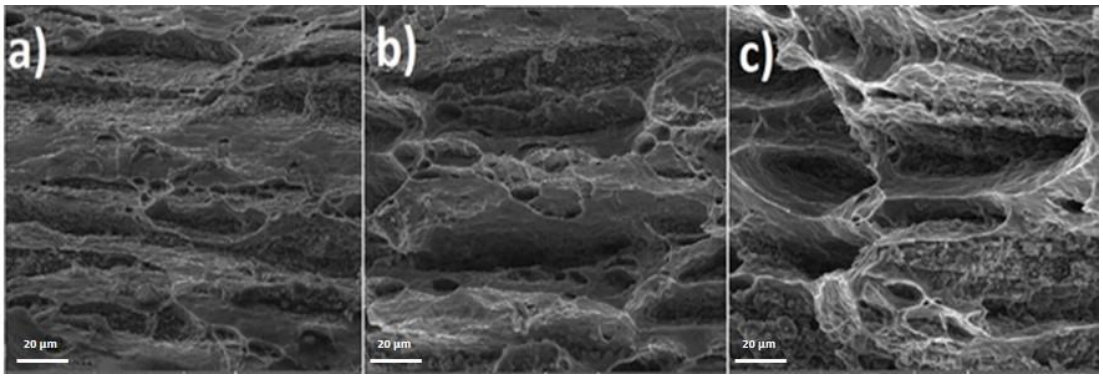

Fig. 7. SEM micrograph of the fracture surface after tensile test at strain rate of 0.01 S^{-1} at different temperatures a) 523K, b) 573K, and c) 623K.

Conclusion

An ultrafine grained Al-0.2wt. % Zr alloy fabricated through 10 cycles of accumulative roll bonding process in this study. The microstructure and mechanical properties of this alloy were investigated. The conclusions can be summarized as follows:

- The UFG material was achieved by accumulative roll bonding process. The fraction of high angle grain boundaries increased during ARB process.
- Temperature and strain rate were effective on elongation to failure in tensile test.
- Increasing the temperature increased the elongation.
- The best result achieved at temperature and strain rate of 623K and 0.01 s^{-1}, respectively, led to maximum elongation of 100% in Al-0.2wt% Zr alloy after 10 cycles ARB.
- Based on the result of tensile test, fracture with more and longer dimples occurred with increasing the temperature. In high temperature dimples were deeper, bigger and longer than low temperature. There was no evidence of necking after failure. Also, maximum elongation observed at 0.01 s^{-1} strain rate and 623K temperature.

References

[1].Borhani, E., Jafarian, H., Shibata, A., Tsuji, N., Mater. Trans., Vol. 53 (2012) pp.1863-1869.

[2].Jafarian, H., Borhani, E., Shibata, A., Terada, D., Tsuji, N., Mater. Sci. Forum, Vol. 667 (2010) pp.361-366.

[3].Borhani, E., Jafarian, H., Adachi, H., Terada, D., Tsuji, N., Mater. Sci. Forum, Vol. 667 (2010) pp.211-216.

[4].Tsuji, N., Encyclopedia of Mate. Sci. & Tech., (2011) pp.1-8.

[5].Borhani, E., Ph.D. thesis, Kyoto University of Japan, 115p. (2012).

[6].Sato, T., Terada, D., Tsuji, N., Mater. Sci. Forum, Vol. 584-586 (2008) pp. 728-733.

[7].Lee, S., Berbon, P. B., Furukawa, M., Horita, Z., Nemoto, M., Tsenev, N. K., Valiev, R. Z., Langdon, T. G.; Mater. Sci. & Eng., Vol. A272 (1999) pp.63-72.

[8].Smolej, A., Skaza, B., Dragojevic, V., JMEPEG Vol. 19 (2010) pp.221–230.

[9].Kawasaki, M., Balasubramanian, N., Langdon, T. G., Mate. Sci. & Eng., Vol. A528 (2011) pp.6624-6629.

[10]. Lee, S., Utsunomiya, A., Akamatsu, H., Neishi, K., Furukawa, M., Horita, Z., Langdon, T.G.; Acta Mater., Vol. 50 (2002) pp.553-564.

[11]. Lee, S., Furukawa, M., Horita, Z., Langdon, T. G.; Mater. Sci. & Eng., Vol. A342 (2003) pp.294-301.

[12]. Borhani, E., Jafarian, H. R., Terada, D., Adachi, H., Tsuji, N., Mater. Trans., Vol. 53 (2012) pp.72-80.

[13]. Borhani, E., Jafarian, H. R., Journal of Ultrafine Grained and Nanostructured Materials, Vol. 47 (2014) pp. 1-7.

[14]. Yaojun, L., Yongan, A., Baiqing, X., Enrique, J. L., Mater. Lett., Vol. 82 (2012) pp.233–236.

[15]. Katsa, S., Dashwood, R., Grimes, R., Jakson, M., Todd, G., Henein, H., Mater. Sci. & Eng., Vol. A444 (2007) pp.291-297.

[16]. Xu, Ch., Furukawa, M., Horita, Z., Langdon, T. G., Acta Mater., Vol. 51 (2003) pp.6139-6149.

[17]. Perevezentsev, V. N., Chuvil, V. N., Kopylov, V. I., Sysoev, A. N., Langdon, T. G., Ann. Chim. Sci. Mat., Vol. 27(3) (2002) pp.99-109.

[18]. Figueiredo, R. B., Kawasaki, M., Langdon, T. G., Rev. Adv. Mater. Sci. Vol. 19 (2009) pp.1-12.

[19]. Kovac, J., Rolf Stock, H., Köhler, B., Bomas, H., Werner Zoch, H.; Surf. & Coat. Thec., Vol. 215 (2013) pp.369-375.

[20]. 20-Wook Kim, H., Bong Kang, S., Tsuji, N., Minamino, Y.; Acta Mater., Vol. 53 (2005) pp.1737–1749.

[21]. Sato, Y. S., Urata, M., Kokawa, H., Ikeda, K.; Scr. Mater., Vol. 47 (2002) pp.869–873.

[22]. Komura, S., Furukawa, M., Horita, Z., Nemoto, M., Langdon, T. G.; Mater. Sci. & Eng., Vol. A297 (2001) pp.111–118.

[23]. Islamgaliev, R. K., Yunusova, N. F., Valiev, R. Z., Tsenev, N. K., Perevezentsev, V. N., Langdon, T. G.; Scr. Mater., Vol. 49 (2003) pp.467–472.

[24]. Dieter, G.E, university of Maryland, "Mechanical Metallurgy", 1928.

[25]. Valiev, R. Z., Salimonenko, D. A., Tsenev, N. K., Berbon, P. B., Langdon, T. G., Scripta Mater. Vol. 37 (1997) pp.1945-1950.

[26]. Tsuji, N., Shiotsuki, K., Saito, Y., Mater. Trans. Vol. 40 (1999) pp.765-771.

[27]. Segal, V. M., Mater. Sci. Eng. Vol. A197 (1995) pp.157-164.

[28]. Ferrasse, S., Segal, V. M., Hartwig, K. T. H., Goforth, R. E., J. Mater. Res. Vol. 12 (1997) 1253-1261.

[29]. Mabuchi, M., Ameyama, K., Iwasaki, H., Higashi, K., Acta Mater. Vol. 47 (1999) 2047-2057.

[30]. Kim, W. J., An, C. W., Kim, Y. S., Hong, S. I., Scripta Mater. Vol. 47 (2002) pp.39-44.

[31]. Matsubara, K., Miyahara, Y., Horita, Z., Langdon, T. G., Acta Mater. Vol. 51 (2003) pp.3073-3084.

[32]. Valiev, R. Z., Islamgaliev, R. K., Alexandrov, I. V., Progress Mater. Sci. Vol. 45 (2000) pp.103-189.

[33]. Baazamat, S., Tajally, M., Borhani, E., Journal of Alloys and Compounds, Vol. 653 (2015) pp.39-46.

[34]. Jafarian, H. R., Borhani, H. R., Shibata, A., Terada, D., Tsuji, N., Journal of materials science, Vol. 46 (2011) pp.4216-4220.

[35]. Jafarian, H. R., Borhani, H. R., Shibata, A., D., Tsuji, N., Journal of Alloys and Compounds, Vol. 577 (2013) pp.668-672 .

[36]. Salimi, A., Borhani, E., Emadoddin, E., Journal of Procedia Materials Science, Vol. 11 (2015) 67-73.

[37]. Azad, B., Borhani, E., Journal of Mining and Metallurgy, Section B: Metallurgy, (2015) (In press).

[38]. Azad, B., Borhani, E., Journal of Materials Engineering and Performance, Vol. 24(12) (2015) pp.4789-4796.

[39]. Langdon, T. G.; Mech. Mater., Vol. 67 (2013) pp.2–8.

[40]. Azad, B., Borhani, E., Mohammadian Semnani, H. R., Kovove Mater., Vol. 54(1) (2016) (In press).